

A possible solution for the faint young Sun paradox: Clues from the exoplanetary data

*Shashanka R. Gurumath*¹, *K. M. Hiremath*^{2,3}, *V. Ramasubramanian*⁴ and *Kinsuk Acharyya*⁵

1. Department of Physics, Bengaluru City University, Bengaluru-560001
2. Indian Institute of Astrophysics, Bengaluru-560034, India; E-mail:hiremath@iiap.res.in
3. #23, Mathru Pithru Krupa, 2nd Cross, 1st Main, BDA Layout, Bikasipura, BSK V Stage, Bengaluru-560111, India
4. Vellore Institute of Technology (VIT), Vellore, India
5. Physical Research Laboratory (PRL), Ahmedabad, India

Abstract

Faint young Sun paradox (FYSP) is one of the interesting problems in solar physics. The present study aims to get a possible solution for the FYSP through sun-like G stars and their exoplanetary systems. Using physical properties of exoplanetary data, an empirical relationship between the rate of mass loss ($\frac{dM}{dt}$) with stellar mass (M_*) and age (t) is obtained. We found mass loss rate varies with stellar mass as $\propto (M_*/M_\odot)^{-3.788}$ and proportional to the age as $\propto t^{-1.25}$, which indicates rate of mass loss is higher during early evolutionary stages. Then we applied mass loss corrections to stellar masses of G-type stars with planets and obtained their initial masses at the early evolutionary stages. Subsequently, we applied these relationships to calculate the mass loss rate and mass of Sun at the early evolutionary stage, which is found to be $\sim 10^{-11}$ solar mass per year and $\sim (1.061 \pm 0.006)$ solar mass respectively. The higher solar mass can probably alleviate the problem of the faint young Sun paradox. Then the estimated initial stellar masses of the host stars are used to obtain a best power law relationship with the planetary masses that supports the hypothesis that the *massive stars harbour massive planets*. Finally, by using the same empirical power law, planetary mass in the vicinity of Sun is estimated to be $\sim (0.84 \pm 0.19)$ Jupiter mass, which is much higher compared to the present solar terrestrial planetary mass. Hence, this study also suggests that there is a missing planetary mass in the vicinity of the Sun, which can solve the FYSP problem.

1 Introduction

The solar system originated from the gravitational collapse of dense interstellar cloud known as the solar nebula which primarily consisted of gas and dust particles (Woolfson, 2014). Many theories are proposed to understand the dynamical evolution of Solar system planets (Nesvorny, 2018) viz., the formation of Jovian planets, the low mass of terrestrial planets by considering migration scenario (Tsiganis et.al. 2005, Walsh et.al. 2011) and, the higher density of the solar nebula (Alibert et.al. 2005, Crida 2009, Mordasini et.al. 2012) during the early history of solar system formation. However, many questions remain unresolved. Faint young Sun paradox (FYSP) is one of such question (Sagan & Mullen 1972, Feulner 2012) which requires a suitable explanation for liquid water on the Earth during the early evolutionary stages.

Several ideas are proposed to solve the FYSP, viz., deviation from the standard solar model (Gaidos et.al. 2000, Shaviv 2003) increase the fraction of greenhouse gases in the early Earth/Mars (Goldblatt & Zahnle 2011, Feulner 2012) etc. One of the promising solutions for FYSP is Sun’s mass during an early stage of evolution must be slightly higher (1.03 - 1.07 M_{\odot} , where M_{\odot} is the mass of the Sun; Section 7.1.2 of Gudel 2007, Minton & Malhotra 2007) compared to the present mass, which can provide a higher level of solar luminosity resulting in more energy output than was predicted.

Present day mass loss rate of Sun is found to be $\sim 10^{-14}M_{\odot}$ /yr, which is estimated only from solar wind. If one estimates initial Sun’s mass by assuming this mass loss rate is constant, it results in increase of 0.05% solar mass that yields negligible increase in Sun’s luminosity. Wood et.al. (2002) obtained a non-linear relationship between mass loss rate and stellar age that suggests mass loss is high during early stages of star formation. In addition, theoretical studies (Drake et.al. 2013 and references there in, Cranmer & Saar 2011) also suggest that Sun mass loss rate is higher ($\sim 10^{-11}M_{\odot}/yr$) during its early evolutionary stages in order to have liquid water on Earth.

Discovery of exoplanets prompted scientific community to understand planet formation in a larger broader scale and compare physical and orbital characteristics (Winn & Fabrycky, 2015) with the Solar system planets. A reasonable subset of exoplanets are around the sun-like G-type stars, therefore in the present study an attempt has been made to understand Faint young Sun paradox by studying the exoplanetary data. We also examined whether present terrestrial mass in the vicinity of the Sun is compatible with mass of exoplanets in the vicinity of their host stars. With these aims in mind, section 2 presents the data and analysis. Section 3 describes the methods to estimate the rate of mass loss of the host stars from the observed data set and, from the empirical rate of mass loss relationship (Jager & Nieuwenhuijzen, 1988). The results and conclusions are presented in section 4.

2 Data and Analysis

For the present study, physical and orbital characteristics of Sun-like G stars and their exoplanets are considered from the website <http://exoplanet.eu/catalog/>. The Sun-like G-type stars in the present study are defined based on the spectral G type provided in the above-mentioned website. Further, we impose the following constraints on the physical properties of stars and exoplanets: (i) consider the host star that has $\leq 50\%$ error in its age, (ii) in order to avoid the ambiguity in considering the brown dwarf candidates, restrict the maximum planetary mass limit to 13 M_J (where M_J is mass of the Jupiter) and, (iii) avoid the binary stellar systems. With these constraints, we left with 114 host stars that have 147 exoplanets. Among 114 host stars, 17 are multi-planetary hosts with 49 planets. The relevant data is given in the Table 1. First column represents the name of an exoplanet. Second and third columns indicate the planetary mass and its error in terms of Jupiter’s mass respectively. Fourth and fifth columns subsequently describe the orbital distance of a planet and its error in terms of AU. Sixth and seventh columns represent the stellar mass and its error in terms of Sun’s mass respectively. Last three columns subsequently indicate the spectral type, age (in Gyrs) and error in age.

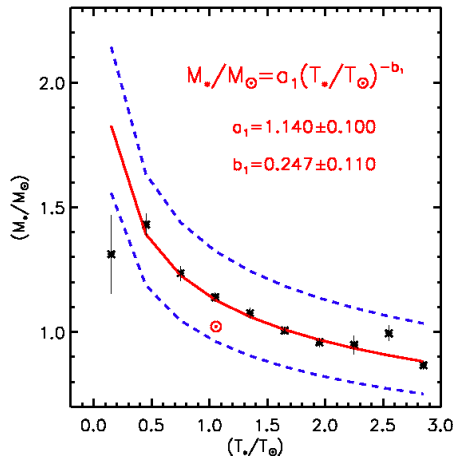


Figure 1: Illustrates the dependence of stellar mass with its age. The continuous line indicates the best power law fit between both the variables and the dashed lines indicate the one sigma error level. \odot symbol indicates the position of the Sun.

One can argue that data bias ((i) high mass planets in the vicinity of stars and (ii) high uncertainties in the stars ages) can lead to misleading results. However, when one examines the data presented in Table 1, following two important facts completely rule out such biases. For example, in addition to hot-Jupiters, the data set also consists of many low-mass planets in the vicinity of their host stars viz., Kepler-10 b, Kepler-11 b, HD 20794 b, HIP 68468 b, etc. In addition, majority of stars in the data set have less than 30% uncertainties in their estimated ages, which help in removing the inconsistencies that arise in estimating the stellar rate of mass loss. Further, one can also notice that the error bars in the stellar and planetary masses are small (on average 10%). Hence, present data set is most appropriate to extract the useful scientific results.

3 Estimation of mass loss from the host stars

The solar type stars lose their mass heavily when they were young (Linsky et.al., 2004) and, the rate of mass loss decreases as the stars evolve (Wood et.al., 2005). This is because, at later evolutionary stages of Sun-like stars, the rotation rate decreases (Hartmann 1985) that results in less magnetic activity. However, mass loss is small for massive stars ($\sim 7M_{\odot}$) in their main sequence stage and increases with the late stage of stellar evolution (Huang et.al. 1990). Hence, stellar mass loss eventually affects the internal structure of a star. The rate of mass loss of host stars ranges from 10^{-14} to $10^{-4} M_{\odot}$ /year (Redgway et.al. 2009) depending upon the different stellar properties viz., stellar mass, luminosity, radius, and temperature. Since the stars are very active in their early evolutionary stages (Hiremath 2009 and references therein, Hiremath 2013), there might have more chance of losing heavy mass from them, that might affect the nearby planets.

3.1 Rate of mass loss estimated from the host stars that have exoplanets

Since we do not know whether the rate of mass loss is same for stars with and without exoplanets, first an attempt is made to understand the variation of stellar masses (that have exoplanets) with their ages. Figure 1 (star's mass M_* and star's age T_* are normalized with the Sun's mass M_\odot and age T_\odot respectively) illustrates a power law relationship between stellar mass and age such that $\frac{M_*}{M_\odot} \sim (\frac{T_*}{T_\odot})^{-0.247}$. In this figure, the x-axis is binned with a size of $0.3 \frac{T_*}{T_\odot}$, and the y-axis represents the average stellar mass in that bin with an error bar estimated from the ratio $\frac{\sigma}{\sqrt{n}}$ (where σ is a standard deviation and n is the number of data points in each bin). Such an empirical power law suggests that the stellar rate of mass loss is high during the initial evolutionary stages.

With the present data set that consists of stellar mass and age and, by making use of numerical differentiation, the rate of mass loss $\frac{d(M_*/M_\odot)}{d(T_*/T_\odot)}$ for each star is estimated. Now onwards, $\frac{M_*}{M_\odot}$ and $\frac{T_*}{T_\odot}$ are represented as M and t respectively. Further, we find that estimated $\frac{dM}{dt}$ fits a power law relation with the stellar mass. By making use of this power law relation, the estimated (see Table 2, second column, second row) rate of mass loss of the Sun is found to be $\sim 10^{-11} M_\odot/\text{yr}$, which matches very well in the range of mass loss computed by the previous studies (Drake et.al. 2013, Cranmer 2017) if one considers mass loss due to coronal mass ejections also.

Careful observation of Table 1 reveals that dataset consists of few giant stars. Since these giant stars have the high rate of mass loss compared to other main sequence stars, one can argue that their presence significantly contribute to the high rate of mass loss of the stars. In order to confirm whether these giants have really affected the rate of mass loss, stellar mass versus age relationship without the giants is illustrated in Figure 2. Further, a relationship is examined between the rate of mass loss of stars (estimated as described above) and their stellar masses that yields the rate of mass loss of Sun to be $\sim 0.9 \times 10^{-12} M_\odot/\text{yr}$ which is almost equal to the previously estimated value. Both these results strongly suggest that contribution due to coronal mass ejections from the Sun substantially increases its present rate of mass loss that is estimated only from the solar wind. One can also notice that Sun's position in both the Figures (1 and 2) is just below the fitted line within one sigma error level. That means, Sun's evolutionary path is no different than the stars evolutionary path that have exoplanets. Hence, Sun might have experienced a major mass loss during its early evolutionary stages that might have kept Earth and Mars atmosphere probably in warm conditions.

Since stellar ages have appreciable but not very high magnitude of error bars, in order to validate the obtained law of mass loss, we have also verified from the data of 42 stars that have accurate stellar mass (average error in stellar mass is $\sim 3.07\%$) and stellar age (average error in stellar age is $\sim 11.80\%$) computed from the asteroseismic method (Metcalf et.al. 2014). Figure 3 illustrates the stellar mass versus age relationship for the stars (with no detected exoplanets) whose properties are accurately determined from the asteroseismic method. The x and y axes are binned as described previous paragraph. Careful observation of Figures 1 - 4 reveals that, during early stellar age ($\leq 0.3 \frac{T_*}{T_\odot}$), stars

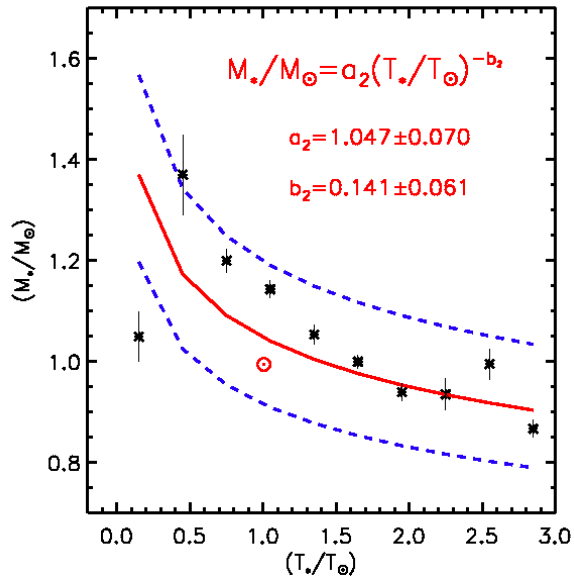


Figure 2: Illustrates the dependence of stellar mass with its age for the dataset without giant stars. The continuous line indicates the best power law fit between both the variables and the dashed lines indicate the one sigma error level. \odot symbol indicates the position of the Sun.

with exoplanets experienced a high rate of mass loss compared to stars without exoplanets. However, cause for the excessive rate of mass loss from the stars with exoplanets during early evolutionary stage is beyond the scope of this study.

3.2 Rate of mass loss estimated from the observations of stars

There is every possibility that, a mismatch between the estimated and observed rate of mass loss of the Sun could be due to not using the observed rate of mass loss of host stars. Hence, the observed (direct estimation) rate of mass loss of host stars, irrespective of whether stars harbour planets or not, are considered from (Cranmer & Saar, 2011). With this data, a power law relationship is obtained between the rate of mass loss of stars and their masses. Using this power law relationship, the present rate of mass loss of the Sun is estimated to be $\sim 0.8 \times 10^{-12} M_\odot/\text{yr}$ which is of the same order ($\sim 10^{-11} M_\odot/\text{yr}$) as estimated from the host star mass-age relationship. For additional check, an empirical rate of mass loss relationship given by [6] is also used to estimate the Sun's present rate of mass loss which is found to be of similar order ($\sim 10^{-14} M_\odot/\text{yr}$; see also Wood et.al. 2005). Obvious reason for the difference of rate of mass loss estimated by Wood et.al. (2005) and our estimation is that, (Wood et.al. 2005) estimate the rate of mass loss due to stellar wind only.

All these three empirical rate of mass loss laws and estimated present Sun's rate of mass loss are presented in the first two rows of Table 2. It is interesting to note that all the three empirical laws suggest power law relationships between the rate of mass loss of stars

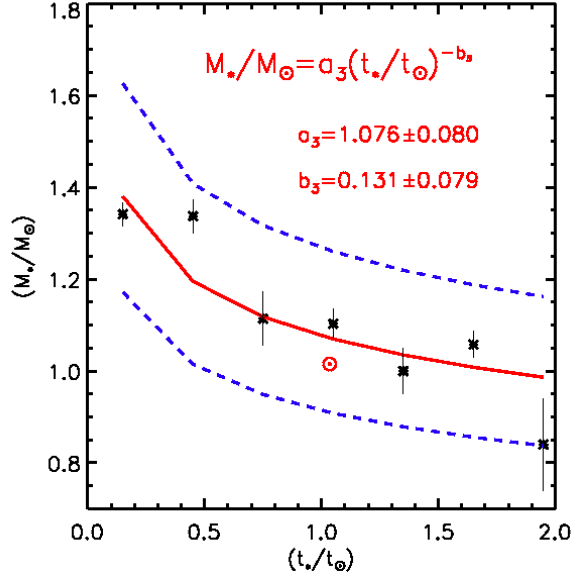


Figure 3: Illustrates the dependence of stellar mass with its age for the stars whose properties are estimated from the asteroseismic method. The continuous line indicates the best power law fit between both the variables and the dashed lines indicate the one sigma error level.

and their respective masses. Hence, it is obvious from these relationships that, high mass stars have a high rate of mass loss.

One can also notice from Table 2 that different mass loss laws yield different initial Sun's mass. Among all the mass loss laws, the estimated uncertainties in the exponents of power laws are least for the mass loss law that is estimated from the host stars data (second column, Table 2). In addition, the Sun's rate of mass loss estimated from this law very well matches with the rate of mass loss estimated by (Drake et.al. 2013). Hence, among these three relationships, best relationship is the one which is derived from the host stars data as described in section 3.1.

3.3 Rate of mass loss as a function of age

Previous study suggests that rotation rate and magnetic activities of stars, that are main reason for mass loss, decrease with stellar age (Vidotto et.al. 2014). Due to high magnetic activity, heavy mass loss occurs in early evolutionary stages of a star. Wood et.al. (2002) theoretically obtained a relation that suggests stellar mass loss decreases with its age. In the present study, by making use of estimated rate of mass loss of stars with exoplanets (as described in previous sections) and their ages, we also obtained a non-linear relationship such that

$$\frac{dM}{dt} = \alpha T_{\star}^{\beta}, \quad (1)$$

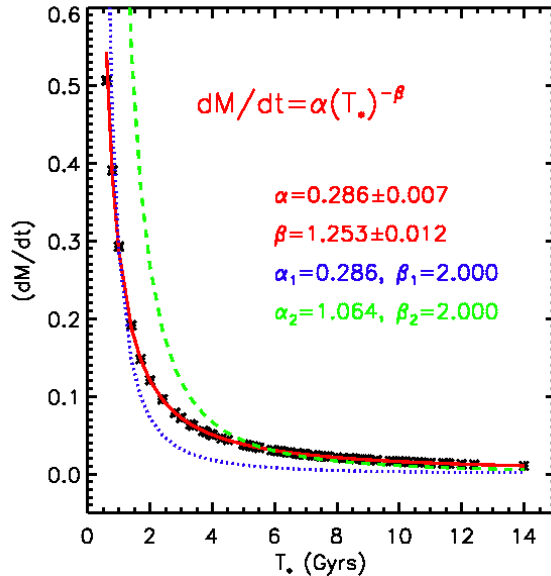


Figure 4: Illustrates the variation of mass loss rate with respect to stellar age. The solid line indicates the best power law fit from the present study, dashed line indicates fit by using exponent from Wood et.al. (2002) and, dotted line indicates fit by exponent from Wood et.al. (2002) and intercept from present study.

where $\alpha = (0.286 \pm 0.007)$, $\beta = (1.253 \pm 0.012)$ and stellar age T_* is in units of Gyrs. Figure 4 illustrates the rate of mass loss as a function of stellar age as given by equation (1). This figure also indicates that mass loss rate is high during early evolutionary phases of star and it decreases with age. We compared our result with the result by Wood et.al. (2002) with different intercepts as mentioned in Figure caption. It shows that power law (equation 1) from the present study fits the data better than the previous study. Furthermore, by using equation (1), rate of mass loss of the Sun is found to be $\sim 2.54 \times 10^{-11} M_{\odot}/yr$ during its early evolutionary stages. Hence, this analysis also supports the results that are obtained in section 3.1.

3.4 Computation of initial stellar mass

With these three empirical power laws (as presented in the first row of Table 2) of rate of mass loss, initial stellar mass M_{ini} can be computed in the following way

$$M_{ini} = M_{pre} + \int_{t_1}^{t_2} \frac{dM}{dt} dt, \quad (2)$$

where M_{pre} is present stellar mass, t_1 and t_2 are initial and present ages of a star respectively.

On the right-hand side (RHS) of equation (2), the second term represents the total mass lost by a star from its initial age t_1 to present age t_2 . Hence, by adding total lost mass to present mass, initial mass M_{ini} of a star can be estimated. In the present study, total

mass lost (numerical integration of the second term in RHS is performed) from the host stars is estimated and is added to the present mass M_{pre} in order to get the initial mass M_{ini} . For estimating total rate of mass loss, initial ages of stars are assigned to be $\sim 50, 60, 70, 80, 90, 100$ and 200 million years and, initial stellar mass is estimated for these ages. However, among all these assigned initial stellar ages, the estimated initial stellar masses converge and saturate at 50 million years than the other assigned ages. Hence, we accept 50 million years as the initial age of a star.

4 Results

After computing the initial stellar masses of the host stars, association between the initial stellar masses and the planetary masses is examined. In the case of multi-planetary systems, all the planetary mass is added that gives the information about the total amount of planetary mass for respective host star. As illustrated in Figure 5 we find that these two parameters are non-linearly (power law) dependent on each other. In Table 3, three power laws that relate the initial host star mass with the planetary mass are presented. In each case, to estimate the initial stellar mass, separate rate of mass loss correction is applied as mentioned in the first column of Table 3.

The power law between the initial stellar mass and planetary mass as illustrated in the Figure 5 suggests that, *the massive stars harbor massive planets in their vicinity*. These results are also consistent with the previous studies of observational (Laws et.al. 2003, Johnson et.al. 2007, Lovis & Mayor 2007, Johnson et.al. 2010) and theoretical inferences (Ida & Lin, 2005). For different spectral type, Lovis & Mayor (2007) present a relationship between exoplanetary mass and stellar mass. However, the present study is different than the previous studies as we have consistently applied the mass loss correction to the stellar mass and also quantitatively estimated the relationship between the stellar mass and the planetary mass.

4.1 Estimation of initial mass of the Sun

Although it is not proper to compare physics of the Solar system with physics of exoplanetary systems, since the Sun has similar physical characteristics such as mass, it is interesting to estimate Sun's lost mass and initial mass from the rate of mass loss relationships (see Table 2, second row). The estimated rate of mass loss of the Sun from the de Jager's empirical formula is no different than the present Sun's rate of mass loss, that is estimated only from the solar wind. This value almost matches with the rate of mass loss estimated by Wood et.al. (2005) if one considers the contribution due to solar wind only. However, from the other two relations, indeed the Sun has an excess rate of mass loss. Especially, if one accepts the rate of mass loss due to coronal mass ejections (Drake et.al. 2013, Cranmer 2017) also, then the rate of mass loss of the Sun increases by $\sim 10^3$ times compared to a rate of mass loss estimated from the solar wind alone and hence inevitably Sun must have an excess initial mass. As we have already mentioned in section 3.2, the best relation between the rate of mass loss and stellar mass is one which

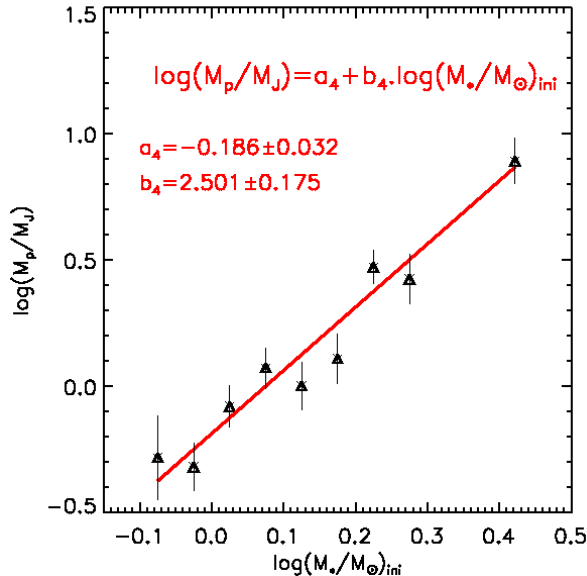


Figure 5: Illustrates the dependence of present mass of the exoplanets with the initial mass of star. The continuous line indicate the best fit line between the planetary mass and initial stellar mass and dashed lines indicate the one sigma error level.

is obtained from the host stars data. Hence, by using rate of mass loss (Table 2, first row and second column) from host stars data we have estimated the Sun's initial mass which is found to be $\sim (1.061 \pm 0.006)M_\odot$. In addition, by making use of equation (1), the Sun's initial mass is estimated to be $\sim (1.05 \pm 0.01)M_\odot$.

It is to be noted that our estimated initial mass is consistent with the initial mass as estimated in the previous studies (Whitmire et.al. 1995, Section 7.1.2 of Gudel 2007). Moreover, the cumulative mass lost by the Sun during its evolution until present age is $0.061 M_\odot$ which is about 1% of the solar mass as recently predicted by Cranmer (2017). Hence, during early evolutionary stages, indeed Sun's mass is slightly higher than the present mass. It is also to be noted that this estimated excess initial mass of the Sun is in the range $(1.03 - 1.07 M_\odot)$; section 7.1.2 of Gudel 2007) of Sun's initial mass that requires Earth to retain the liquid water. This astrophysical solution is a possible reason for alleviating the long-standing problem of faint young Sun paradox.

4.2 Estimation of initial planetary mass in the vicinity of Sun

With the calculated Sun's initial mass and making use of empirical relationships as presented in Table 3, estimated average planetary mass in the vicinity of Sun is found to be $\sim (0.84 \pm 0.18)M_J$. In contrast, the present total planetary mass (that includes masses of all the terrestrial planets and asteroids) in the vicinity of Sun is $\sim 0.006 M_J$ (~ 2 earth mass). One can notice that the difference between estimated and observed planetary mass of the terrestrial planets suggests that a substantial amount of planetary mass is missing in the vicinity of Sun. Careful observation of stars within the spectral type G provides an

evidence of huge ($\sim 0.8 M_J$) planetary mass in their vicinity. Further, if we concentrate on stars that belong to spectral type G2 (similar to Sun), the average planetary mass within their vicinity is found to be $\sim 1.3 M_J$. In addition, there are eight stars in the present dataset with similar mass ($\pm 0.2 M_\odot$, along with spectral type G2) as that of the Sun whose average planetary mass within their vicinity is $\sim 0.7 M_J$. Among these eight stars, minimum planetary mass within vicinity is $\sim 0.3 M_J$ for the star WASP-126 and, maximum planetary mass is $\sim 1.1 M_J$ for the star WASP-95. These all evidences suggest that the Sun is in deficiency of planetary mass within its vicinity.

Probably during early phase of the Solar system evolution, some part of that missing mass might have accreted onto the Sun like other stars (Matt et.al. 2012) or some part might have blown off to space due to intense solar radiation (X-rays, EUV radiations) or protoplanetary disk might have blown off by photoevaporation (Mitchell & Stewart, 2010) or part of this missing mass might have migrated outwards (Walsh et.al. 2011) from the vicinity of Sun during the early history of Solar system formation. Another possibility could be due to dynamical barriers imposed by the gas giants (Izidoro et.al. 2015) for migration of super earths, although Kepler data do not support such a migration scenario (Chatterjee & Tan 2015). Hence, further clear understanding of deficiency in the present planetary mass in the vicinity of Sun from the perspectives of theory and analysis of the observed physical characteristics of exoplanetary data is necessary.

Since the Sun-like stars were very active during early evolutionary stages (Wood et.al. 2005, Hiremath 2009, Hiremath 2013, combined mass loss due to solar wind and coronal mass ejections might have affected the mass of the nearby planets. As for estimated initial planetary mass $(0.84 \pm 0.18)M_J$ in the vicinity of Sun, since the planets also lose mass due to intense radiation from the host stars, with a caveat we have to conclude that, unambiguous planetary mass loss correction is also necessary. Presently, the planetary mass loss is not well understood and mass loss correction for the planets is beyond the scope of this study. However, in case mass loss correction for the planets is also applied, estimated initial planetary mass might further increases and aggravates the deficiency of planetary mass in the vicinity of Sun.

5 Conclusions

To conclude this study, physical and orbital characteristics of Sun-like G stars and their exoplanets are used to seek a possible solution for the faint young Sun paradox. Having a dataset of sun-like stars distributed over a range of stellar ages, a relationship between stellar mass and age is obtained that suggests mass stellar mass decreases with stellar age. By using this relationship and having knowledge of stellar age, rate of mass loss of each star is estimated. By estimating the rate of mass loss of each star,

- we obtained a non-linear relationship between the rate of mass loss of host star and its mass such that $(dM/dt) \propto (M_\star/M_\odot)^{3.79}$.
- We obtained a relationship between mass loss of a star and its age such that

$(dM/dt) \propto (T_*/T_\odot)^{-1.25}$ that suggests, stars experience high mass loss rate during their early evolutionary stages.

- Rate of mass loss of the Sun during early evolutionary stage is estimated to be $\sim 10^{-11} M_\odot/\text{yr}$. This high value of rate of mass loss can keep liquid water on Earth, that is also suggested by previous studies (Cranmer 2017, Minton & Malhotra 2007, Whitmire et.al. 1995).
- By using Sun's rate of mass loss its initial mass is estimated to be $\sim (1.061 \pm 0.006) M_\odot$, that can alleviate the faint young Sun paradox.
- We acquire a non-linear relationship between initial stellar mass and planetary mass that suggests massive stars harbour massive planets.
- From the relationship between initial stellar mass and their exoplanetary mass, initial planetary mass in the vicinity of Sun is estimated to be $\sim (0.84 \pm 0.18) M_J$, in excess of planetary mass concentrated at the present epoch. The excess solar planetary mass lost is conjectured with different views.

Table 1: Physical and orbital characteristics of exoplanets and their host stars

Name	M_p (M_J)	δM_p (M_J)	a (AU)	δa AU	M_* (M_\odot)	δM_* (M_\odot)	Spectral Type	T_* (Gyrs)	δT_* (Gyrs)
24 Sex b	1.990	0.380	1.333	0.009	1.540	0.080	G5	2.70	0.40
24 Sex c	0.860	0.220	2.080	0.020	1.540	0.080	G5	2.70	0.40
47 Uma b	2.530	0.060	2.100	0.020	1.030	0.050	G0V	7.40	1.90
47 Uma c	0.540	0.073	3.600	0.100	1.030	0.050	G0V	7.40	1.90
47 Uma d	1.640	0.480	11.600	2.900	1.030	0.050	G0V	7.40	1.90
61 Vir b	0.016	0.001	0.050	0.000	0.950	0.030	G5V	8.96	3.00
61 Vir c	0.057	0.003	0.217	0.000	0.950	0.030	G5V	8.96	3.00
61 Vir d	0.072	0.008	0.476	0.001	0.950	0.030	G5V	8.96	3.00
CoRoT-12 b	0.917	0.065	0.040	0.001	1.078	0.072	G2V	6.30	3.10
CoRoT-16 b	0.535	0.085	0.061	0.001	1.098	0.078	G5V	6.73	2.80
CoRoT-17 b	2.430	0.160	0.046	0.001	1.040	0.100	G2V	10.70	1.00
CoRoT-23 b	2.800	0.250	0.047	0.004	1.140	0.080	G0V	7.20	1.00
CoRoT-25 b	0.270	0.040	0.057	0.003	1.090	0.050	G0V	5.20	1.30
CoRoT-26 b	0.520	0.050	0.052	0.001	1.090	0.060	G8IV	8.60	1.80
CoRoT-28 b	0.484	0.087	0.059	0.003	1.010	0.140	G8/9IV	12.00	1.50
HAT-P-13 b	0.850	0.038	0.042	0.001	1.220	0.100	G4	5.00	0.80
HAT-P-15 b	1.946	0.066	0.096	0.001	1.013	0.043	G5	6.80	1.60
HAT-P-21 b	4.063	0.161	0.049	0.001	0.947	0.042	G3	10.20	2.50
HAT-P-22 b	2.147	0.061	0.041	0.001	0.916	0.035	G5	12.40	2.60
HAT-P-23 b	2.090	0.110	0.023	0.000	1.130	0.050	G5	4.00	1.00
HAT-P-28 b	0.626	0.037	0.043	0.001	1.025	0.047	G3	6.10	1.90
HAT-P-38 b	0.267	0.020	0.052	0.001	0.886	0.044	G	10.10	4.80
HATS-11 b	0.850	0.120	0.046	0.001	1.000	0.060	G0	7.70	1.60
HATS-19 b	0.427	0.071	0.058	0.001	1.303	0.830	G0	3.94	0.50
HATS-25 b	0.613	0.042	0.051	0.001	0.994	0.035	G	7.50	1.90
HATS-28 b	0.672	0.087	0.041	0.001	0.929	0.036	G	6.20	2.80
HATS-29 b	0.653	0.063	0.054	0.001	1.032	0.049	G	5.50	1.70
HATS-8 b	0.138	0.019	0.046	0.001	1.056	0.037	G2V	5.10	1.70
HD 10180 c	0.041	-	0.064	0.001	1.060	0.050	G1V	4.30	0.50
HD 10180 d	0.036	-	0.128	0.002	1.060	0.050	G1V	4.30	0.50
HD 10180 e	0.078	-	0.269	0.004	1.060	0.050	G1V	4.30	0.50
HD 10180 f	0.075	-	0.492	0.007	1.060	0.050	G1V	4.30	0.50
HD 10180 g	0.067	-	1.422	0.026	1.060	0.050	G1V	4.30	0.50
HD 10180 h	0.202	-	3.400	0.110	1.060	0.050	G1V	4.30	0.50
HD 102365 b	0.050	0.008	0.460	0.040	0.850	-	G2V	9.00	3.00
HD 104985 b	8.300	-	0.950	-	1.600	-	G9 III	2.95	0.65
HD 106270 b	11.000	0.800	4.300	0.400	1.320	0.092	G5	4.30	0.60
HD 10697 b	6.830	0.984	2.160	0.120	1.150	0.030	G5 IV	6.90	0.60
HD 109271 b	0.054	0.004	0.079	0.001	1.047	0.024	G5V	7.30	1.20
HD 109271 c	0.076	0.007	0.196	0.003	1.047	0.024	G5V	7.30	1.20
HD 109749 b	0.280	0.016	0.063	-	1.200	0.100	G3 IV	10.30	2.90
HD 11506 b	3.440	0.470	2.430	0.120	1.190	0.100	G0V	5.40	1.60
HD 11506 c	0.820	0.500	0.639	0.017	1.190	0.100	G0V	5.40	1.60
HD 117207 b	2.060	-	3.780	-	1.070	-	G8VI/V	6.68	2.20
HD 11755 b	6.500	1.000	1.080	0.040	0.900	0.100	G5	10.20	1.30
HD 12648 b	2.900	0.400	0.540	0.020	1.200	0.100	G5	4.50	1.00
HD 132406 b	5.610	-	1.980	-	1.090	0.050	G0V	6.40	0.80
HD 134987 b	1.590	0.020	0.810	0.020	1.070	0.080	G5 V	9.70	3.70
HD 134987 c	0.820	0.030	5.800	0.500	1.070	0.080	G5 V	9.70	3.70
HD 136418 b	2.000	0.100	1.320	0.030	1.330	0.090	G5	4.00	1.00
HD 13931 b	1.880	0.150	5.150	0.290	1.020	0.020	G0	8.40	2.00
HD 14067 b	7.800	0.700	3.400	0.100	2.400	0.200	G9 III	0.69	0.20
HD 149026 b	0.357	0.011	0.042	0.000	1.300	0.100	G0 IV	2.00	0.80
HD 149143 b	1.330	-	0.052	-	1.100	0.100	G0 IV	7.60	1.20
HD 154672 b	5.020	0.170	0.600	0.170	1.060	0.090	G3IV	9.28	2.36
HD 16175 b	4.770	0.370	2.148	0.076	1.350	0.090	G0	5.30	1.00
HD 162004 b	1.530	0.100	4.430	0.040	1.190	0.070	G0V	3.30	1.30
HD 16417 b	0.069	0.007	0.140	0.010	1.180	0.040	G1V	4.30	0.80
HD 165155 b	2.890	0.230	1.130	0.040	1.020	0.050	G8V	11.00	4.00
HD 168443 b	7.659	0.097	0.293	0.001	0.995	0.019	G5	9.80	1.00
HD 170469 b	0.670	-	2.240	-	1.140	0.020	G5IV	6.70	1.10
HD 171028 b	1.980	-	1.320	-	0.990	0.080	G0	8.00	2.00
HD 17156 b	3.195	0.033	0.162	0.002	1.275	0.018	G0	3.38	0.47
HD 175607 b	0.028	0.003	-	-	0.710	0.010	G6V	10.32	1.58
HD 187085 b	0.750	-	2.050	-	1.220	0.100	G0 V	3.30	1.20
HD 18742 b	2.700	0.300	1.920	0.050	1.600	0.110	G9IV	2.30	0.50
HD 188015 b	1.260	-	1.190	-	1.090	-	G5IV	6.20	2.32
HD 20794 b	0.008	0.001	0.120	0.002	0.850	0.040	G8V	14.00	5.00
HD 20794 c	0.007	0.001	0.203	0.003	0.850	0.040	G8V	14.00	5.00
HD 20794 d	0.015	0.002	0.349	0.006	0.850	0.040	G8V	14.00	5.00
HD 209458 b	0.690	0.017	0.047	0.000	1.148	0.022	G0V	4.00	2.00
HD 212771 b	2.300	0.400	1.220	0.300	1.150	0.080	G8IV	6.00	2.00
HD 219077 b	10.390	0.090	6.220	0.090	1.050	0.020	G8V	8.90	0.30
HD 219828 b	0.066	0.004	0.045	-	1.240	-	G0IV	5.80	1.20
HD 221585 b	1.610	0.140	2.306	0.081	1.190	0.120	G8IV	6.20	0.50
HD 222155 b	1.900	0.530	5.100	0.700	1.130	0.110	G2V	8.20	0.70
HD 224693 b	0.710	-	0.233	-	1.330	0.100	G2IV	2.00	0.50
HD 24040 b	4.010	0.490	4.920	0.380	1.180	-	G0	6.68	1.52
HD 30177 b	8.070	0.120	3.580	0.010	1.050	0.080	G8 V	11.60	2.20
HD 30177 c	3.000	0.300	6.990	0.420	1.050	0.080	G8 V	11.60	2.20
HD 34445 b	0.790	0.070	2.070	0.020	1.070	0.020	G0	8.50	2.00
HD 38529 b	0.930	0.110	0.131	0.001	1.480	0.050	G4 IV	3.28	0.30
HD 4308 b	0.040	0.005	0.118	0.009	0.850	-	G5 V	7.10	3.00
HD 4313 b	2.300	0.200	1.190	0.030	1.720	0.120	G5 D	2.00	0.50
HD 43691 b	2.490	-	0.240	-	1.380	0.050	G0IV	2.80	0.80
HD 5319 b	1.940	-	1.750	-	1.560	0.180	G5IV	2.40	0.68
HD 5319 c	1.150	0.080	2.071	0.013	1.560	0.180	G5IV	2.40	0.68

Table 1 continued

Name	M_p (M_J)	δM_p (M_J)	a (AU)	δa AU	M_* (M_\odot)	δM_* (M_\odot)	Spectral Type	T_* (Gyrs)	δT_* (Gyrs)
HD 72659 b	3.150	0.140	4.740	0.080	0.950	2.000	G2 V	6.50	1.50
HD 72892 b	5.450	0.370	0.228	0.008	1.020	0.050	G5V	8.00	3.00
HD 74156 b	1.778	0.020	0.291	0.003	1.240	0.040	G1V	3.70	0.40
HD 74156 c	7.997	0.095	3.820	0.044	1.240	0.040	G1V	3.70	0.40
HD 75898 b	2.510	-	1.190	-	1.280	0.130	G0	3.80	0.80
HD 82886 b	1.300	0.100	1.650	0.060	1.060	0.074	G0	7.00	2.00
HD 9174 b	1.110	0.140	2.200	0.090	1.030	0.050	G8IV	9.00	3.00
HD 96167 b	0.680	0.180	1.300	0.070	1.310	0.090	G5D	3.80	1.00
HIP 11915	0.990	0.060	4.800	0.100	1.000	-	G5V	4.00	0.60
HIP 68468 b	0.011	-	0.029	-	1.050	0.010	G3V	5.90	0.40
HIP 68468 c	0.094	-	0.665	-	1.050	0.010	G3V	5.90	0.40
K2-24 b	0.066	0.017	0.154	0.002	1.120	0.050	G9V	5.00	1.80
K2-24 c	0.085	0.022	0.247	0.004	1.120	0.050	G9V	5.00	1.80
K2-60 b	0.426	0.037	0.045	0.003	0.970	0.070	G4V	10.00	3.00
K2-99 b	0.970	0.090	0.159	0.006	1.600	0.100	G0 IV	2.40	0.60
KELT-8 b	0.874	0.066	0.045	0.009	1.211	0.066	G2V	5.40	0.50
Kepler-10 b	0.010	0.001	0.016	0.000	0.910	0.021	G	10.60	1.50
Kepler-10 c	0.054	0.005	0.241	0.001	0.910	0.021	G	10.60	1.50
Kepler-11 b	0.005	0.003	0.091	0.003	0.950	0.100	G	8.00	2.00
Kepler-11 c	0.009	0.005	0.106	0.004	0.950	0.100	G	8.00	2.00
Kepler-11 d	0.022	0.004	0.159	0.005	0.950	0.100	G	8.00	2.00
Kepler-11 e	0.030	0.006	0.194	0.007	0.950	0.100	G	8.00	2.00
Kepler-11 f	0.006	0.002	0.250	0.009	0.950	0.100	G	8.00	2.00
Kepler-11 g	0.950	0.950	0.462	0.016	0.950	0.100	G	8.00	2.00
Kepler-12 b	0.431	0.041	0.055	0.001	1.166	0.054	G0	4.00	0.40
Kepler-20 b	0.030	0.004	0.046	0.001	0.912	0.035	G8	8.80	2.70
Kepler-20 c	0.040	0.007	0.094	0.002	0.912	0.035	G8	8.80	2.70
Kepler-20 d	0.031	0.011	0.350	0.010	0.912	0.035	G8	8.80	2.70
Kepler-20 e	0.009	-	0.063	0.001	0.912	0.035	G8	8.80	2.70
Kepler-20 f	0.045	-	0.139	0.003	0.912	0.035	G8	8.80	2.70
Kepler-20 g	0.062	0.011	0.205	0.002	0.912	0.035	G8	8.80	2.70
Kepler-4 b	0.082	0.012	0.045	0.001	1.223	0.091	G0	4.50	1.50
Kepler-41 b	0.490	0.090	0.029	0.001	0.940	0.090	G2V	7.40	3.40
Kepler-412 b	0.939	0.085	0.029	0.001	1.167	0.091	G3V	5.10	1.70
Kepler-43 b	3.230	0.190	0.044	0.001	1.320	0.090	G0V/G0IV	2.80	0.80
Kepler-44 b	1.020	0.070	0.045	0.001	1.190	0.100	G2IV	6.95	1.70
Kepler-66 b	0.310	0.070	0.135	0.001	1.038	0.044	G0V	1.00	0.17
Kepler-67 b	0.310	0.060	0.117	0.001	0.865	0.034	G9V	1.00	0.17
Kepler-75 b	9.900	0.500	0.080	0.005	0.880	0.060	G8V	6.00	3.00
Kepler-77 b	0.430	0.032	0.045	0.001	0.950	0.040	G5V	7.50	2.00
Pr 0211 b	1.880	0.020	0.031	0.001	0.935	0.013	G9	0.79	0.03
Pr 0211 c	7.950	0.250	5.800	1.400	0.935	0.013	G9	0.79	0.03
WASP-102 b	0.624	0.045	0.040	0.000	1.167	0.035	G0	0.60	0.30
WASP-110 b	0.515	0.064	0.045	0.001	0.892	0.072	G9	8.60	3.50
WASP-112 b	0.880	0.120	0.038	0.001	0.807	0.073	G6	10.60	3.00
WASP-119 b	1.230	0.083	0.036	0.001	1.020	0.060	G5	8.00	2.50
WASP-12 b	1.404	0.099	0.022	0.001	1.350	0.140	G0	1.70	0.80
WASP-126 b	0.280	0.040	0.044	0.001	1.120	0.060	G2	6.40	1.60
WASP-127 b	0.180	0.020	0.052	0.001	1.080	0.030	G5	11.41	1.80
WASP-133 b	1.160	0.090	0.034	0.001	1.160	0.080	G4	6.80	1.80
WASP-157 b	0.576	0.093	0.052	0.001	1.260	0.120	G2V	1.00	0.30
WASP-19 b	1.114	0.040	0.016	0.000	0.904	0.045	G8V	11.50	2.70
WASP-26 b	1.028	0.021	0.039	0.000	1.120	0.030	G0	6.00	2.00
WASP-37 b	1.800	0.170	0.043	0.001	0.849	0.040	G2	11.00	4.00
WASP-46 b	2.101	0.073	0.024	0.000	0.956	0.034	G6V	1.40	0.60
WASP-5 b	1.637	0.082	0.027	0.000	1.000	0.060	G5	3.00	1.40
WASP-8 b	2.244	0.093	0.080	0.001	1.033	0.050	G6	4.00	1.00
WASP-95 b	1.130	0.040	0.034	0.001	1.110	0.090	G2	2.40	1.00
XO-1 b	0.900	0.070	0.048	0.000	1.000	0.030	G1V	4.50	2.00
XO-5 b	1.077	0.037	0.048	0.000	0.880	0.030	G8V	8.50	0.80

References

- [1] Y. Alibert, C. Mordasini, W. Benz, and C. Winisdoerffer. Models of giant planet formation with migration and disc evolution. *Astronomy and Astrophysics*, 434:343–353, April 2005.
- [2] S. Chatterjee and J. C. Tan. Vulcan Planets: Inside-out Formation of the Innermost Super-Earths. *Astrophys. J. Letters*, 798:L32, January 2015.
- [3] S. R. Cranmer. Mass-loss Rates from Coronal Mass Ejections: A Predictive Theoretical Model for Solar-type Stars. *Astrophys. J.*, 840:114, May 2017.

Table 2: Rate of Mass loss of stars with planets

	Mass loss obtained from host star data	Mass loss obtained from observed data	Mass loss obtained from empirical relation
Rate of mass loss $\frac{dM}{dt}$	$c_1 \left(\frac{M_\star}{M_\odot}\right) 3.788 \pm 0.190$	$c_2 \left(\frac{M_\star}{M_\odot}\right) 3.974 \pm 1.394$	$10^{-8.158} \left[\frac{\left(\frac{L_\star}{L_\odot}\right)^{1.768}}{\left(T_{eff}\right)^{1.676}}\right]$
Sun's rate of mass loss	$1.361 \times 10^{-11} M_\odot/\text{yr}$	$8.090 \times 10^{-13} M_\odot/\text{yr}$	$3.4435 \times 10^{-15} M_\odot/\text{yr}$
Initial M_\odot	$1.061 \pm 0.006 M_\odot$	$1.003 \pm 0.006 M_\odot$	$1.000015 M_\odot$

where $c_1=(0.062\pm 0.003)$, $c_2=(0.003\pm 0.002)$, M_\star - mass of the star, τ_\odot - age of Sun.

Note: (i) The results from second column are obtained from the exoplanetary dataset as explained in section 3.1, results from third column are obtained from observed mass loss data from the [4] as explained in section 3.2, and the results from the last column are obtained by using empirical formula from [6].

Table 3: Relationship between host stars initial mass and planetary mass

Corrections applied	$\left(\frac{M_p}{M_J}\right)$ versus initial $\left(\frac{M_\star}{M_\odot}\right)_{ini}$ relationships	Missing planetary mass in the vicinity of Sun
Host star data correction	$\log\left(\frac{M_p}{M_J}\right) = (-0.191 \pm 0.045) + (2.366 \pm 0.220)\log\left(\frac{M_\star}{M_\odot}\right)_{ini}$	$0.738 \pm 0.172 M_J$
Observed mass loss correction	$\log\left(\frac{M_p}{M_J}\right) = (-0.116 \pm 0.041) + (2.560 \pm 0.223)\log\left(\frac{M_\star}{M_\odot}\right)_{ini}$	$0.887 \pm 0.191 M_J$
Empirical mass loss correction	$\log\left(\frac{M_p}{M_J}\right) = (-0.102 \pm 0.041) + (2.522 \pm 0.233)\log\left(\frac{M_\star}{M_\odot}\right)_{ini}$	$0.914 \pm 0.198 M_J$
Average initial planetary mass	$0.846 \pm 0.187 M_J$	

- [4] S. R. Cranmer and S. H. Saar. Testing a Predictive Theoretical Model for the Mass Loss Rates of Cool Stars. *Astrophys. J.*, 741:54, November 2011.
- [5] A. Crida. Minimum Mass Solar Nebulae and Planetary Migration. *Astrophys. J.*, 698:606–614, June 2009.
- [6] C. de Jager, H. Nieuwenhuijzen, and K. A. van der Hucht. Mass loss rates in the Hertzsprung-Russell diagram. *Astronomy and Astrophysics, supplement*, 72:259–289, February 1988.
- [7] J. J. Drake, O. Cohen, S. Yashiro, and N. Gopalswamy. Implications of Mass and Energy Loss due to Coronal Mass Ejections on Magnetically Active Stars. *Astrophys. J.*, 764:170, February 2013.
- [8] G. Feulner. The faint young Sun problem. *Reviews of Geophysics*, 50:RG2006, May 2012.
- [9] E. J. Gaidos, M. Güdel, and G. A. Blake. The Faint Young Sun Paradox: An observational test of an alternative solar model. *Geophysics Research Letters*, 27:501–503, February 2000.
- [10] C. Goldblatt and K. J. Zahnle. Faint young Sun paradox remains. *Nature*, 474:E1, June 2011.
- [11] M. Güdel. The Sun in Time: Activity and Environment. *Living Reviews in Solar Physics*, 4, December 2007.
- [12] L. Hartmann. Mass loss from solar-type stars. *Solar Physics*, 100:587–597, October 1985.

- [13] K. M. Hiremath. Solar Forcing on the Changing Climate. *Sun and Geosphere*, 4:16–21, October 2009.
- [14] K. M. Hiremath. *Seismology of the Sun: Inference of Thermal, Dynamic and Magnetic Field Structures of the Interior*. 2013.
- [15] R. Q. Huang, S. Y. Jiang, Z. W. Han, and Y. Lie. Evolution of a mass-losing star of 7 solar masses. *Astronomy and Astrophysics*, 229:99–103, March 1990.
- [16] S. Ida and D. N. C. Lin. Dependence of Exoplanets on Host Stars’ Metallicity and Mass. *Progress of Theoretical Physics Supplement*, 158:68–85, 2005.
- [17] A. Izidoro, S. N. Raymond, A. Morbidelli, F. Hersant, and A. Pierens. Gas Giant Planets as Dynamical Barriers to Inward-Migrating Super-Earths. *Astrophys. J. Letters*, 800:L22, February 2015.
- [18] J. A. Johnson, K. M. Aller, A. W. Howard, and J. R. Crepp. Giant Planet Occurrence in the Stellar Mass-Metallicity Plane. *Publications of the ASP*, 122:905–915, August 2010.
- [19] J. A. Johnson, R. P. Butler, G. W. Marcy, D. A. Fischer, S. S. Vogt, J. T. Wright, and K. M. G. Peek. A New Planet around an M Dwarf: Revealing a Correlation between Exoplanets and Stellar Mass. *Astrophys. J.*, 670:833–840, November 2007.
- [20] C. Laws, G. Gonzalez, K. M. Walker, S. Tyagi, J. Dodsworth, K. Snider, and N. B. Suntzeff. Parent Stars of Extrasolar Planets. VII. New Abundance Analyses of 30 Systems. *Astronomical Journal*, 125:2664–2677, May 2003.
- [21] J. L. Linsky, B. E. Wood, H.-R. Müller, and G. P. Zank. Mass Loss of Solar-like Dwarf Stars and the Young Sun. In A. K. Dupree and A. O. Benz, editors, *Stars as Suns : Activity, Evolution and Planets*, volume 219 of *IAU Symposium*, page 898, January 2004.
- [22] C. Lovis and M. Mayor. Planets around evolved intermediate-mass stars. I. Two substellar companions in the open clusters NGC 2423 and NGC 4349. *Astronomy and Astrophysics*, 472:657–664, September 2007.
- [23] S. P. Matt, G. Pinzón, T. P. Greene, and R. E. Pudritz. Spin Evolution of Accreting Young Stars. II. Effect of Accretion-powered Stellar Winds. *Astrophys. J.*, 745:101, January 2012.
- [24] T. S. Metcalfe, O. L. Creevey, G. Doğan, S. Mathur, H. Xu, T. R. Bedding, W. J. Chaplin, J. Christensen-Dalsgaard, C. Karoff, R. Trampedach, O. Benomar, B. P. Brown, D. L. Buzasi, T. L. Campante, Z. Çelik, M. S. Cunha, G. R. Davies, S. Deheuvels, A. Derekas, M. P. Di Mauro, R. A. García, J. A. Guzik, R. Howe, and MacGregor. Properties of 42 Solar-type Kepler Targets from the Asteroseismic Modeling Portal. *Astrophys. J. Supplement*, 214:27, October 2014.

- [25] D. A. Minton and R. Malhotra. Assessing the Massive Young Sun Hypothesis to Solve the Warm Young Earth Puzzle. *Astrophys. J.*, 660:1700–1706, May 2007.
- [26] T. R. Mitchell and G. R. Stewart. Evolution of the Solar Nebula and Planet Growth Under the Influence of Photoevaporation. *Astrophys. J.*, 722:1115–1130, October 2010.
- [27] C. Mordasini, Y. Alibert, W. Benz, H. Klahr, and T. Henning. Extrasolar planet population synthesis . IV. Correlations with disk metallicity, mass, and lifetime. *Astronomy and Astrophysics*, 541:A97, May 2012.
- [28] D. Nesvorný. Dynamical Evolution of the Early Solar System. *Annual Review of Astron and Astrophys*, 56:137–174, September 2018.
- [29] S. Ridgway, J. Aufdenberg, M. Creech-Eakman, N. Elias, S. Howell, D. Hutter, M. Karovska, S. Ragland, E. Wishnow, and M. Zhao. Quantifying Stellar Mass Loss with High Angular Resolution Imaging. In *astro2010: The Astronomy and Astrophysics Decadal Survey*, volume 2010 of *Astronomy*, 2009.
- [30] C. Sagan and G. Mullen. Earth and Mars: Evolution of Atmospheres and Surface Temperatures. *Science*, 177:52–56, July 1972.
- [31] Nir J. Shaviv. Toward a solution to the early faint sun paradox: A lower cosmic ray flux from a stronger solar wind. *Journal of Geophysical Research: Space Physics*, 108(A12), 2003.
- [32] K. Tsiganis, R. Gomes, A. Morbidelli, and H. F. Levison. Origin of the orbital architecture of the giant planets of the Solar System. *Nature*, 435:459–461, May 2005.
- [33] A. A. Vidotto, S. G. Gregory, M. Jardine, J. F. Donati, P. Petit, J. Morin, C. P. Folsom, J. Bouvier, A. C. Cameron, G. Hussain, S. Marsden, I. A. Waite, R. Fares, S. Jeffers, and J. D. do Nascimento. Stellar magnetism: empirical trends with age and rotation. *MNRAS*, 441:2361–2374, July 2014.
- [34] K. J. Walsh, A. Morbidelli, S. N. Raymond, D. P. O’Brien, and A. M. Mandell. A low mass for Mars from Jupiter’s early gas-driven migration. *Nature*, 475:206–209, July 2011.
- [35] D. P. Whitmire, L. R. Doyle, R. T. Reynolds, and J. J. Matese. A slightly more massive young Sun as an explanation for warm temperatures on early Mars. *Journal of Geophysics Research*, 100:5457–5464, March 1995.
- [36] Joshua N. Winn and Daniel C. Fabrycky. The occurrence and architecture of exoplanetary systems. *Annual Review of Astronomy and Astrophysics*, 53(1):409–447, 2015.
- [37] B. E. Wood, H.-R. Müller, G. P. Zank, and J. L. Linsky. Measured Mass-Loss Rates of Solar-like Stars as a Function of Age and Activity. *Astrophys. J.*, 574:412–425, July 2002.

- [38] B. E. Wood, H.-R. Müller, G. P. Zank, J. L. Linsky, and S. Redfield. New Mass-Loss Measurements from Astrospheric Ly α Absorption. *Astrophys. J. Letters*, 628:L143–L146, August 2005.
- [39] M. Woolfson. *The Formation of the Solar System: Theories Old and New (2ND Edition)*. World Scientific Publishing Co, September 2014.